

Multispectral optoacoustic tomography enables assessment of disease activity in paediatric inflammatory bowel disease

Adrian P. Regensburger^{a,b,*}, Markus Eckstein^c, Matthias Wetzl^d, Roman Raming^{a,b}, Lars-Philip Paulus^{a,b}, Adrian Buehler^{a,b}, Emmanuel Nedoschill^{a,b}, Vera Danko^{a,b}, Jörg Jüngert^a, Alexandra L. Wagner^b, Alexander Schnell^a, Aline Rückel^a, Ulrich Rother^e, Oliver Rompel^d, Michael Uder^d, Arndt Hartmann^c, Markus F. Neurath^f, Joachim Woelfle^a, Maximilian J. Waldner^f, André Hoerning^{a,1}, Ferdinand Knieling^{a,b,1}

^a Department of Paediatrics and Adolescent Medicine and German Center Immunotherapy (DZI), University Hospital Erlangen, Friedrich-Alexander-Universität (FAU) Erlangen-Nürnberg, Erlangen, Germany

^b Paediatric Experimental and Translational Imaging Laboratory (PETI-Lab), Department of Paediatrics and Adolescent Medicine, University Hospital Erlangen, Friedrich-Alexander-Universität (FAU) Erlangen-Nürnberg, Erlangen, Germany

^c Institute of Pathology, University Hospital Erlangen, Friedrich-Alexander-Universität (FAU) Erlangen-Nürnberg, Erlangen, Germany

^d Department of Radiology, University Hospital Erlangen, Friedrich-Alexander-Universität (FAU) Erlangen-Nürnberg, Erlangen, Germany

^e Department of Vascular Surgery, University Hospital Erlangen, Friedrich-Alexander-Universität (FAU) Erlangen-Nürnberg, Erlangen, Germany

^f Department of Medicine 1 and German Center Immunotherapy (DZI), University Hospital Erlangen, Friedrich-Alexander-Universität (FAU) Erlangen-Nürnberg, Erlangen, Germany

ARTICLE INFO

Keywords:

Optoacoustic imaging
Multispectral optoacoustic tomography
Paediatric inflammatory bowel disease

ABSTRACT

Multispectral optoacoustic tomography (MSOT) allows non-invasive molecular disease activity assessment in adults with inflammatory bowel disease (IBD). In this prospective pilot-study, we investigated, whether increased levels of MSOT haemoglobin parameters corresponded to inflammatory activity in paediatric IBD patients, too. 23 children with suspected IBD underwent MSOT of the terminal ileum and sigmoid colon with standard validation (e.g. endoscopy). In Crohn's disease (CD) and ulcerative colitis (UC) patients with endoscopically confirmed disease activity, MSOT total haemoglobin (HbT) signals were increased in the terminal ileum of CD (72.1 ± 13.0 a.u. vs. 32.9 ± 15.4 a.u., $p = 0.0049$) and in the sigmoid colon of UC patients (62.9 ± 13.8 a.u. vs. 35.1 ± 16.3 a.u., $p = 0.0311$) as compared to controls, respectively. Furthermore, MSOT haemoglobin parameters correlated well with standard disease activity assessment (e.g. SES-CD and MSOT HbT ($r_s = 0.69$, $p = 0.0075$)). Summarizing, MSOT is a novel technology for non-invasive molecular disease activity assessment in paediatric patients with inflammatory bowel disease.

1. Introduction

The incidence of inflammatory bowel diseases (IBD) in children is rising and already accounts for 25% of all IBD patients [1], with an yearly incidence of up to 23 per 100.000 children [2]. For paediatric patients, in addition to the two main entities - Crohn's disease (CD) and ulcerative colitis (UC)- a third class -Inflammatory bowel disease unclassified (IBD-U)- exists. Besides common symptoms such as abdominal pain, haematochezia and diarrhoea, children are significantly affected

by malnutrition, followed by growth delay and developmental disorders [3]. Therefore, early therapeutical interventions are essential for disease control and mucosal healing [4]. However, criteria for mucosal healing are still a matter of debate, and definitions of subsequent endpoints in paediatric IBD (PIBD) trials remain to be more clearly defined [5]. Standard procedures to assess IBD activity in clinical routine care combine routine laboratory chemistry, especially faecal calprotectin [6], ultrasound [7], and MR-enterography [8], providing reasonable precision for the evaluation of treatment response and detection of

* Correspondence to: Paediatric Experimental and Translational Imaging Laboratory (PETI-Lab), Department of Paediatrics and Adolescent Medicine, Friedrich-Alexander-Universität (FAU) Erlangen-Nürnberg, Loschggestraße 15, Erlangen 91054, Germany.

E-mail address: adrian.regensburger@uk-erlangen.de (A.P. Regensburger).

¹ Authors contributed equally to the work

<https://doi.org/10.1016/j.pacs.2023.100578>

Received 8 September 2023; Received in revised form 1 November 2023; Accepted 29 November 2023

Available online 1 December 2023

2213-5979/© 2023 Published by Elsevier GmbH. This is an open access article under the CC BY-NC-ND license (<http://creativecommons.org/licenses/by-nc-nd/4.0/>).

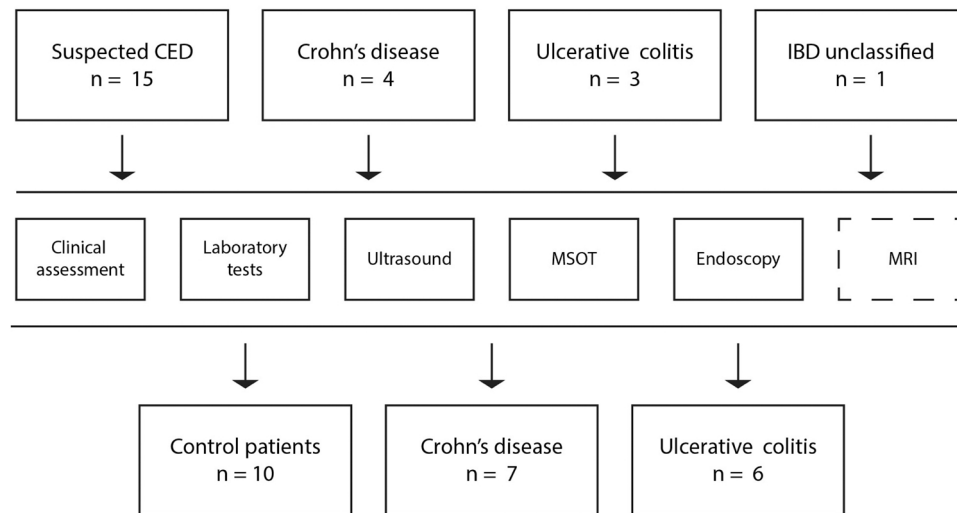


Fig. 1. Study flow chart. Paediatric patients with suspected or diagnosed CED (Crohn's disease (CD), Ulcerative colitis (UC) or inflammatory bowel disease unclassified (IBD-U)) were investigated by clinical assessment, laboratory blood and stool tests, B-mode and colour Doppler ultrasound, Multispectral optoacoustic tomography (MSOT), endoscopy (ileocolonoscopy) and, if indicated, MR-enterography. For statistical analyses three groups (control patients, CD and UC) were formed, with IBD-U patients being added to the UC group.

flares. Furthermore, the gold standard for disease assessment, invasive endoscopic procedures, including biopsies for histology, are still frequently required to confirm the extent of the disease. Not surprisingly, they are recommended as the primary endpoint of randomized controlled trials [5]. To avoid invasive procedures and the risks of sedation in early childhood, novel diagnostic modalities to assess disease activity in IBD are highly needed. Handheld multispectral optoacoustic tomography (MSOT) has demonstrated the potential to monitor adult inflammatory bowel disease [9,10]. MSOT is based on the expansion of molecules by light and the consecutive detection of the emitted pressure waves [11]. For translational studies, resolution of the imaging devices can be scaled from mesoscopic to tomographic for different applications [12,13]. By using multiple wavelengths and distinct absorption patterns, dedicated molecules can be quantified using spectral unmixing techniques [14]. One of the main absorbers in human tissues is haemoglobin, which can be used as an optoacoustic imaging (OAI) surrogate biomarker for inflammation in various diseases [15].

In adult patients with Crohn's disease, different MSOT haemoglobin levels allowed stratification according to the disease activity and to define remission [9,10]. Furthermore, OAI systems are developed into (capsule) endoscopic devices [16–18] and might be used to assess upper gastrointestinal tract involvement in patients with Crohn's disease. However, up to date, no OAI data regarding paediatric IBD exists. We hypothesise, that severity of intestinal disease activity can be assessed by MSOT in children with ulcerative colitis and Crohn's disease, too.

2. Material and methods

2.1. Investigator-initiated trial protocol

An investigator-initiated trial was conducted between 31st of March 2021 and 12th of December 2022. The study was registered at clinicaltrials.gov (NCT04650867), approved by the local ethics committee (351_20 B) and performed in adherence to the Declaration of Helsinki. Patients were recruited at the Department of Paediatric Gastroenterology at the University Hospital Erlangen during routine appointments. Informed consent of all legal guardians was obtained. Inclusion criteria were suspected or diagnosed inflammatory bowel disease, scheduled colonoscopy and age between two and 18 years. Exclusion criteria were pregnancy, nursing mothers, patients with a need for continuous cardiopulmonary monitoring, tattoos in the field of view, subcutaneous fat

tissue with a depth over 3 cm and missing informed consent.

Three groups of patients were enrolled: 1. Suspected or diagnosed Crohn's disease (CD), 2. Suspected or diagnosed ulcerative colitis (UC), 3. Suspected or diagnosed unclassified inflammatory bowel disease (IBD-U). Thereafter, all patients underwent routine clinical scoring, laboratory chemistry (blood and stool), B-mode and colour Doppler ultrasound, Multispectral optoacoustic tomography combined with reflected-ultrasound computed tomography (MSOT/RUCT), endoscopy (ileo-colonoscopy) and, if indicated, Magnetic resonance (MR)-enterography. After final diagnosis, all patients were assigned to one of the following groups for further statistical analysis: 1. Control patients (no diagnosis of CED), 2. CD patients or 3. UC patients. The one IBD-U patient was assigned to the group of UC patients, according to the disease pattern.

2.2. Clinical assessment

Patients were interviewed regarding their clinical symptoms. In cases of CD the Paediatric Crohn's disease activity Index (PCDAI) was used [19,20] with PCDAI ≤ 10 indicating remission, PCDAI 10–29 suggesting mild disease and PCDAI ≥ 30 at least moderate disease activity. For UC/IBD-U the Paediatric Ulcerative Colitis Activity Index (PUCAI) [21] with PUCAI < 10 indicating no, 10–34 mild, 35–64 moderate, and ≥ 65 severe disease activity was implemented.

2.3. Clinical Chemistry

Routine blood samples (EDTA, lithium-heparin and serum) were collected and analysed for haemoglobin levels (g/dl), platelets ($\times 10^3/\mu\text{l}$), total leukocytes ($\times 10^3/\mu\text{l}$), c-reactive protein (CrP) (mg/l), and erythrocyte sedimentation rate (ESR) (mm/one hour); other laboratory parameters are not shown. Furthermore, stool samples were analysed for faecal calprotectin ($\mu\text{g/g}$). All analyses were performed routinely at the clinical chemistry laboratory of the Department of Paediatrics and Adolescent Medicine at the University Hospital Erlangen.

2.4. B-mode and colour Doppler Ultrasound

B-mode and colour Doppler ultrasound were performed by physicians (APR and JJ) certified by the paediatric section of the German Society of Ultrasound in Medicine. For imaging, either a GE LOGIQ E9

Table 1
Demographic characteristics and multi-modality assessments.

	n	Controls n = 10	n	Crohn's disease n = 7	n	Ulcerative colitis n = 6
Females (n)	10	2 (20%)	7	4 (57%)	6	3 (50%)
Age (years)	10	10.8 ± 4.3	7	12.3 ± 4.6	6	14.8 ± 2.6
Age (month)	10	133.7 ± 51.3	7	154.3 ± 56.5	6	185.2 ± 31.7
Height (cm)	10	149.8 ± 24.2	7	155.0 ± 27.2	6	165.3 ± 11.3
Weight (kg)	10	41.7 ± 17.0	7	45.3 ± 13.1	6	48.8 ± 9.4
BMI (kg/m ²)	10	17.8 ± 3.0	7	18.6 ± 1.8	6	17.8 ± 2.8
Clinical assessment						
PCDAI (score)	10	10.0 ± 9.1	7	19.6 ± 13.3	-	-
PUCAI (score)	10	14.5 ± 13.6	-	-	6	38.3 ± 20.7
Laboratory assessment						
ESR (mm/h)	10	7.0 ± 4.7	6	52.3 ± 43.2	5	28.8 ± 23.5
CrP (mg/l)	10	1 ± 0.8	7	19.7 ± 29.4	6	4.6 ± 5.1
Haemoglobin (g/dl)	10	14.1 ± 1.5	7	12.3 ± 1.8	6	12.7 ± 1.7
Platelets (x10 ³ /μl)	10	336.5 ± 71.5	7	423.7 ± 112.6	6	307.5 ± 60.4
Leucocytes (x10 ³ /μl)	10	7.9 ± 2.9	7	9.2 ± 1.8	6	6.5 ± 1.4
Calprotectin (μg/g stool)	10	243.7 ± 384.1	6	1068.1 ± 995.7	6	477.9 ± 379.7
Multi-modality imaging assessment						
Ultrasound-TI (Limberg score)	10	0.2 ± 0.6	7	1.9 ± 1.5	6	0.3 ± 0.5
Ultrasound-SI (Limberg score)	10	0.0 ± 0.0	7	0.4 ± 0.8	6	0.7 ± 0.8
Endoscopy (SES-CD score)	10	0.0 ± 0.0	6	8.3 ± 8.0	-	-
Endoscopy (UCEIS score)	10	0.1 ± 0.3	-	-	6	5.2 ± 1.5
MRI (sMaria score)	2	0.5 ± 0.7	5	1.6 ± 1.8	4	3.3 ± 5.9
Microscopic assessment						
Histology-TI (Riley score for CD)	10	0.3 ± 0.7	5	8.4 ± 5.6	5	1.0 ± 1.7
Histology-TI (Nancy score)	10	0.0 ± 0.0	5	2.4 ± 1.5	5	0.8 ± 1.3
Histology-SI (Riley score for UC)	10	0.5 ± 0.5	6	4.8 ± 4.2	6	11.0 ± 7.1
Histology-SI (Nancy score)	10	0.0 ± 0.0	6	2.0 ± 1.7	6	2.8 ± 1.8
Safety assessment						
SAEs (n)	10	0 (0%)	7	0 (0%)	6	0 (0%)

PCDAI = Paediatric Crohn's Disease Activity Index, PUCAI = Paediatric Ulcerative Colitis Activity Index, ESR = Erythrocyte Sedimentation Rate, CrP = C-reactive protein, TI = terminal ileum, SI = sigmoid colon, SES-CD = simple endoscopic score for Crohn's disease, UCEIS = Ulcerative Colitis Endoscopic Index of Severity, sMARIA = simplified Magnetic Resonance Index of Activity, SAE = Serious Adverse Event; Data in number (n), percentage (%) or mean ± standard deviation.

(GE Medical Systems Ultrasound, LLC, Wauwatosa, USA) or a GE LOGIQ E10 (GE Medical Systems Ultrasound, LLC, Wauwatosa, USA) equipped with linear L2–9 and ML6–15 probes were used. Herein we analysed the terminal ileum and the sigmoid colon as follows: bowel wall thickness (in millimetres (mm)) and vascularization pattern (non, mild, moderate or severe), summarized as modified Limberg score (0 = no bowel wall thickening, 1 = bowel wall thickness ≥3 mm, no hypervascularization, 2 = + short-distance hypervascularization, 3 = + long-distance hypervascularization, 4 = + hypervascularization reaching the mesentery) [22].

2.5. Multispectral optoacoustic tomography/reflected-ultrasound computed tomography (MSOT/RUCT)

A single MSOT/RUCT prototype hybrid ultrasound imaging system (MSOT Acuity Echo, iThera Medical GmbH, Munich, Germany) was used as described previously [10,23–25] and as provided by the manufacturer: “A tunable optical parametric oscillator (OPO) pumped by an Nd:YAG laser provides excitation pulses with a duration of 4 ns at wavelengths tunable from 660 nm to 1300 nm at a repetition rate of 25 Hz and a peak pulse energy of 35 mJ at 730 nm. A fiber bundle was integrated into the ultrasound detector. The optical fluence was tuned to be below 8.3 mJ/cm² at 730 nm to ensure adherence with ANSI limits of maximum permissible exposure (MPE). For ultrasound detection, 256 ultrasound transducers with a center frequency of 4 MHz (100% bandwidth in receive mode), organized in a concave array of 125 degree angular coverage and a radius of curvature of 4 cm, are used. In addition to optoacoustic imaging the system is also capable of interleaved reflection-mode ultrasound computed tomography (RUCT) image acquisition [26]. For pulse-echo image generation in the RUCT acquisition mode, an ultrasound imaging platform was used that consolidates a 128-channel beamformer and a function of triggered acquisition for synchronizing ultrasound and optoacoustic image streams. The pulser was programmed to generate bipolar 1-cycle pulse trains with a peak-to-peak voltage of 20 V and frequency of 6 MHz (60% bandwidth), and the reflected signals were digitized at 20MS/s sampling rate. Ultrasound images were acquired with a frame rate of 10 frames/sec.” The maximum imaging depth is ~ 2.5 cm. The simultaneous RUCT imaging allows identification of the bowel wall. Thereafter MSOT signals were captured in short videos (approx. 10–20 s). During video acquisition the probe was held without movement to reduce motion artefacts. In addition, as provided in the system and by the manufacturer “the imaging system was equipped with a motion indicator based on selective frame averaging algorithm. The cross-correlation between OA images at 800 nm from consecutive cycles is calculated and used as indicator of motion. The same algorithm was used in postprocessing for image averaging to increase signal-to-noise ratio. Images with motion were excluded from averaging. No motion correction was applied.”

For safety reason all examinations were carried out in a laser (class 4 device) safety approved room with external laser indicators. All patients and attending persons had to wear safety goggles (protection wavelength 660–1400 nm and DIR LB4 (OD4)) during imaging. The skin of the scanning region was visually investigated after imaging and all adverse events were documented.

The data was then transferred to the institutional data servers and processed with cLabs software (V2.66, iThera Medical GmbH, Munich, Germany). Reconstruction of images was done by backprojection algorithm. A polygonal ROI was placed according to the bowel wall on the RUCT image and in respect of the optoacoustic signal. ROIs were checked by a second, blinded reader (FK). Single wavelengths (SWL) 715 nm, 730 nm, 760 nm, 800 nm and 850 nm were used for spectral unmixing of MSOT parameters deoxygenated haemoglobin (Hb) and oxygenated haemoglobin (HbO₂) by linear regression algorithm and presented as arbitrary units (a.u.). The MSOT parameters total haemoglobin (HbT) and oxygen saturation (mSO₂) are derived by post hoc calculations (HbT = HbR + HbO₂; mSO₂ = HbO₂ / HbT with exclusion of the 0.5% lowest HbT signals).

2.6. Magnetic resonance enterography

Patients with indication for MR-enterography within the clinical work pertaining the suspected/diagnosed IBD were examined. MRI scanners with a field strength of 1.5 (Magnetom Aeara, Siemens Healthineers) or 0.55 Tesla (Magnetom Free.Max, Siemens Healthineers) were used. Weight-dependent (0.1 ml/kg body weight) contrast media (Gadobutrol, concentration 1 mmol/ml) was applied for contrast-enhanced images. MRIs were evaluated by a board-certified radiologist

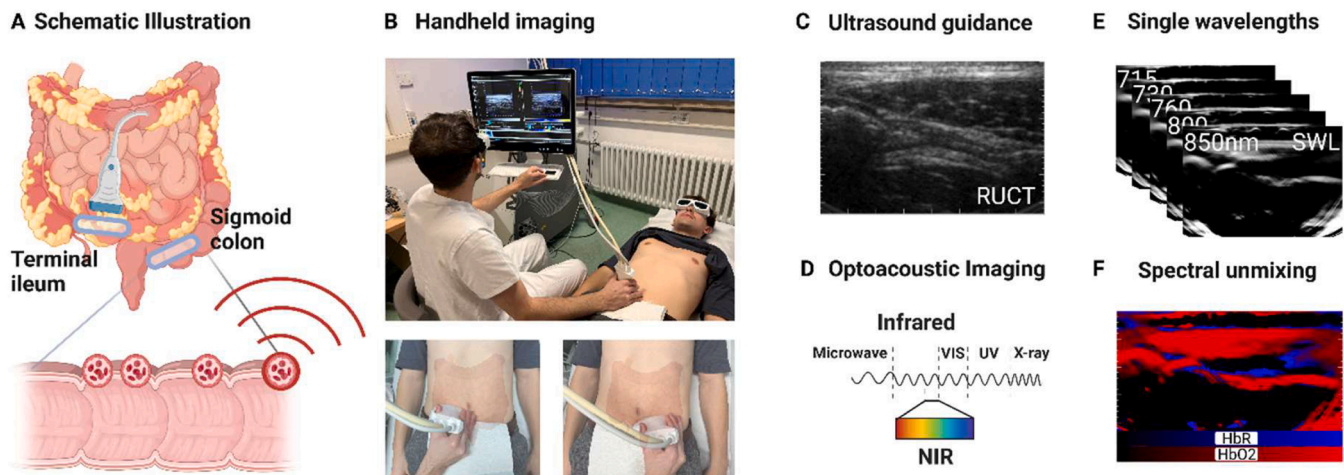


Fig. 2. Multispectral optoacoustic imaging of the intestine. (A+B) The intestinal wall of the terminal ileum and sigmoid colon were investigated using handheld hybrid Multispectral Optoacoustic Tomography (MSOT)/ Reflected Ultrasound Computed Tomography (RUCT). Schematic illustration and bedside MSOT imaging set-up of the investigated regions of interest (blue ellipsis over the terminal ileum and the sigmoid colon). Created with biorender.com, (C) RUCT imaging allows real-time guidance of the investigator during bedside examinations to identify the bowel wall. (D-F) MSOT uses pulsed laser light in the near infrared window of light (NIR) to induce thermoelastic expansion of molecules and records the emitted pressure waves. By using distinct wavelengths specific molecules, such as deoxygenated (HbR) and oxygenated (HbO₂) haemoglobin, they can be quantified and visualized by spectral unmixing algorithms. Created with BioRender.com.

(MW) according to sMARIA Score for mural thickening, oedema, fat stranding, and mucosal ulcerations as follows: sMARIA = (1 × thickness > 3 mm) + (1 × edema) + (1 × fatstranding) + (2 × ulcers) [27,28].

2.7. Endoscopy-Ileocolonoscopy

All endoscopies were performed in analgesedation. A Pentax Medical EPK-i7010 system (PENTAX Europe GmbH, Hamburg, Germany) with endoscopes (EC3490Li or EC3890LK), adapted to the respective patient's age and body habit, was used. Patients with diagnosed CD were scored according to the simplified endoscopic activity score for Crohn's disease (SES-CD) [29] as follows: size of ulcers (0–3), ulcerated surface (0–3), affected surface (0–3), and stenosis (0–3) for each segment reaching from 0 to 56. A score between 0 and 2 was regarded as clinical remission, 3–6 as mildly active, 7–15 as moderately active, and ≥ 16 as severely active [30]. Patients with diagnosed UC were scored according to Ulcerative Colitis Endoscopic Index of Severity (UCEIS) [31]. The score was adapted for vascular pattern (0–2), bleeding (0–3), and erosions/ulcers (0–3). The following cut-offs were used to define remission (UCEIS 0–1), mild (UCEIS 2–4), moderate (UCEIS 5–6), and severe (UCEIS 7–8) disease [32]. Patients with suspected IBD were scored according to both SES-CD and UCEIS score.

2.8. Histopathology

Routine biopsy specimens were taken during colonoscopy and further embedded and processed in the Institute of Pathology at the University Hospital Erlangen. The samples were stained according to standard protocols for haematoxylin and eosin (HE). Two different scorings (Riley and Nancy score) of histopathological sections were performed by a board-certified pathologist (ME) as follows: Riley score adapted for CD with following nine features on a zero to four scale, respectively: Lymphocyte aggregates, acute inflammatory cell infiltrates (neutrophils), crypt abscesses, mucin depletion, surface epithelial integrity, chronic inflammatory cell infiltrates, crypt architectural irregularities, granuloma and eosinophils [10,33]. A total score from 0 to 4 reflecting histological remission, ≥ 5 active disease, 5–9 low activity, 10–18 moderate activity, ≥ 19 high activity; the Riley score was adapted for UC with following six features on a zero to four scale, respectively: Lymphocyte aggregates, acute inflammatory cell infiltrates

(neutrophils), crypt abscesses, mucin depletion, surface epithelial integrity, chronic inflammatory cell infiltrate [33]. Nancy score with the following four features: Predicted global visual evaluation, ulcerations, acute inflammatory cell infiltrates and chronic inflammatory infiltrates. Nancy score grading was zero to four [34].

2.9. Statistical analyses

Patient characteristics are given as number and percentage (%) or mean and standard deviation (SD). No sample size calculation was performed due to the pilot character of the study. Due to the small number of patients in each group, all data was regarded as not normally distributed. For comparisons between all three groups Kruskal-Wallis test with Dunn's correction for multiple comparisons was used, and for comparison between two groups the Mann-Whitney test was used. Correlations are given with the respective Spearman correlation coefficient (rs). All tests were two-tailed, and a p-value < 0.05 indicated statistical significance. Analyses were performed with GraphPad Prism software (Prism 9, San Diego, California, USA).

3. Results

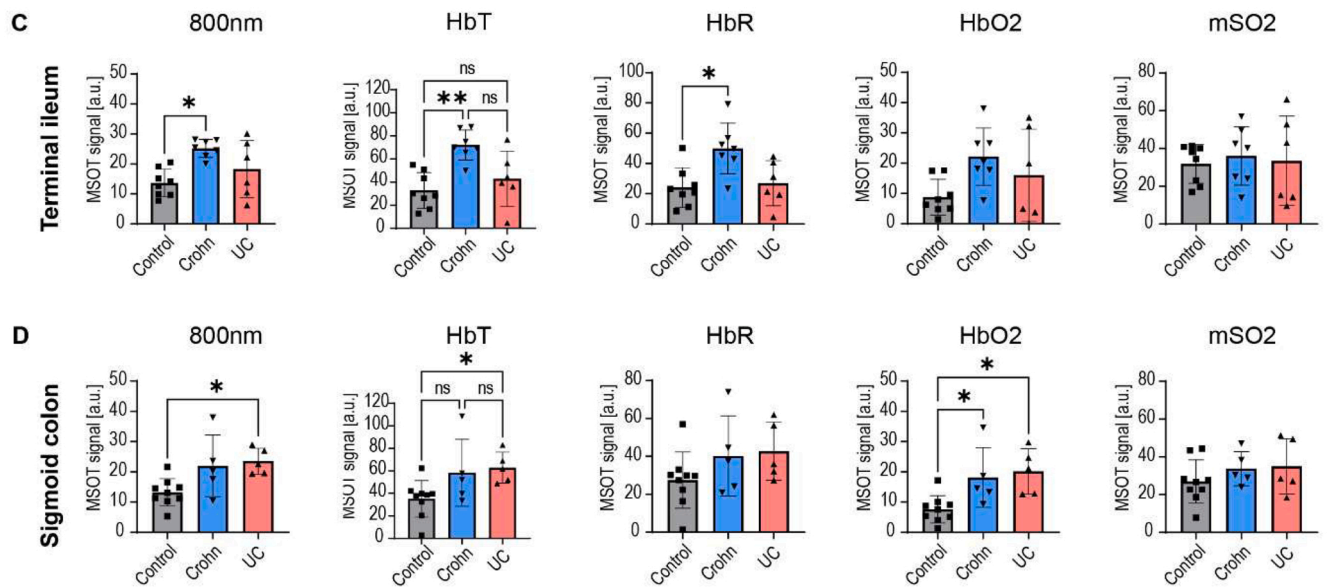
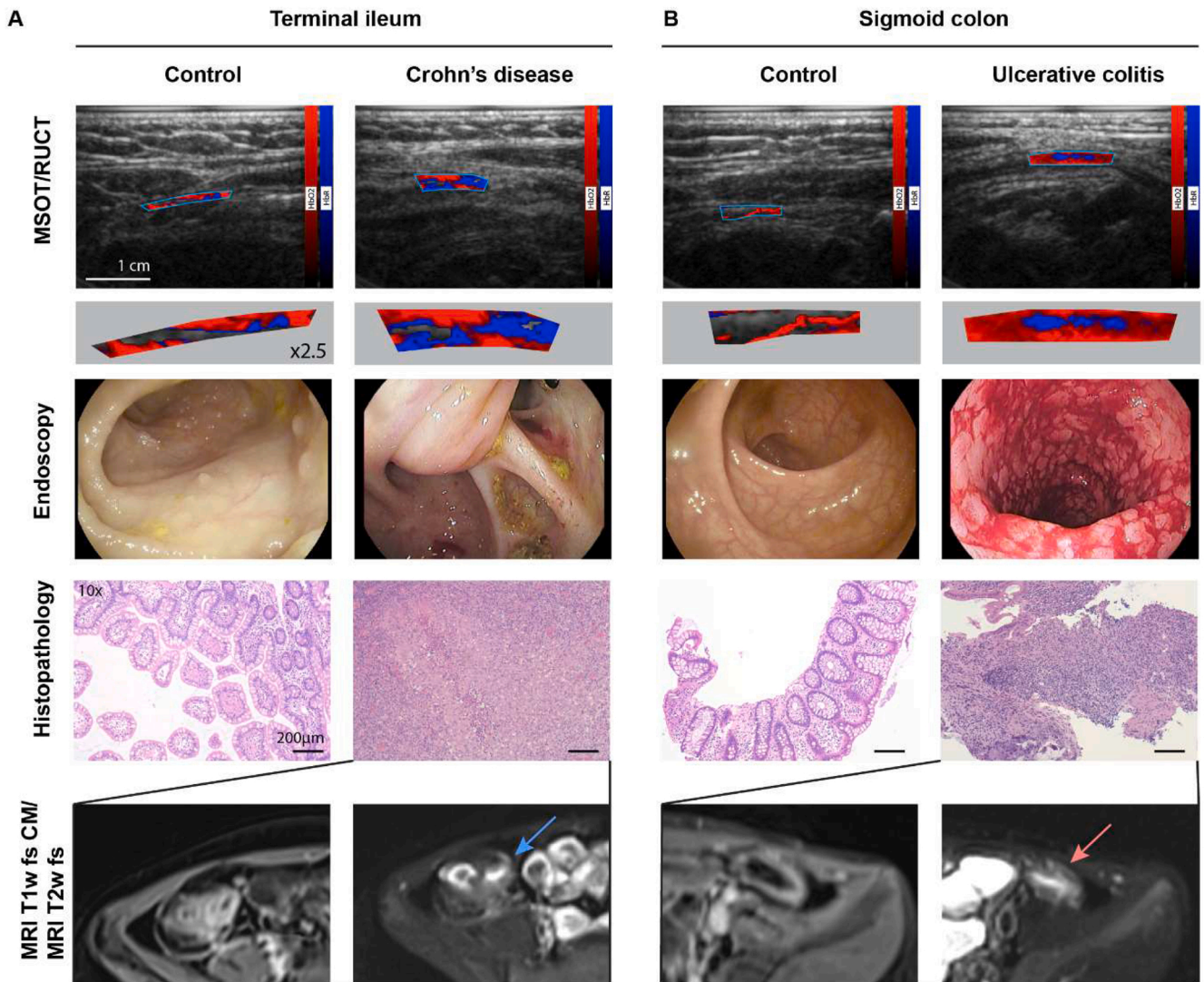
3.1. Patient characteristics

A total of 23 patients were included in the study, comprising 15 patients with suspected IBD, four with CD, three with UC and 1 with IBDU. After diagnostic workup, patients were assigned as control (total of n = 10: juvenile polyp n = 2, post-infectious colitis n = 2, allergic colitis n = 5 and drug-induced colitis n = 1), CD (n = 7) or UC (n = 6) patients (Fig. 1). Demographic characteristics are displayed in Table 1. Briefly, mean ± SD age of control patients was 10.8 ± 4.3 years, 12.3 ± 4.6 of CD and 14.8 ± 2.6 years of UC patients. Height, weight and BMI did not show statistically significant differences between groups (all p > 0.05). All patients underwent clinical, laboratory (blood and stool), ultrasound, MSOT, and endoscopic examinations and, if indicated, MR-enterography for disease assessment (see Table 1).

3.2. Disease assessment

3.2.1. Clinical assessment

Clinical assessment by PCDAI did not show statistically significant



(caption on next page)

Fig. 3. Multispectral optoacoustic imaging and quantification of paediatric inflammatory bowel diseases. (A+B) Displayed are exemplary MSOT/RUCT images, endoscopy with histopathology, and MRI fat-saturated T1- and T2-weighted images of a 7 year old control patient (polypectomy), a 17 year old patient with Crohn's disease (CD) and a 10 year old patient with ulcerative colitis (UC). Hybrid MSOT/RUCT allows real-time guidance to allocate the bowel wall and region of interest (ROI) placement. MSOT parameters for deoxygenated (HbR) and oxygenated (HbO₂) haemoglobin are coloured blue and red and the respective signals are visualized within the ROI. 2.5-fold visualizations of the MSOT signals within the ROI are given to enlighten signal differences. MSOT haemoglobin signals are higher in CD and UC compared to control patients. This is in line with markedly increased signs for inflammation in endoscopy, histopathology (H&E staining) and MR-enterography. The terminal ileum of the CD patient was stenosed and the histopathology derived from surgical ileocecal resection. Scale bar indicates 1 cm in MSOT/RUCT and 200 μ m in histopathology images. (C+D) MSOT signal intensities for single wavelength 800 nm (SWL800nm), total haemoglobin (HbT), deoxygenated haemoglobin (HbR), oxygenated haemoglobin (HbO₂) and oxygen saturation (mSO₂). Signal intensities were compared between control, CD and UC patients for the terminal ileum (C) and sigmoid colon (D). $p < 0.05$ was regarded as statistically significant (* <0.05 ** <0.01).

differences between controls and CD patients (10.0 ± 9.1 vs. 19.6 ± 13.3 , $p = 0.0614$). Of all CD patients, two were in remission, three in mild and 2 in moderate to severe disease activity. PUCAI scores revealed significantly different scores between control and UC patients (14.5 ± 13.6 vs. 38.3 ± 20.7 , $p = 0.0174$). Of all UC patients, three had mild, two had moderate and one had high disease activity.

3.2.2. Laboratory assessment (blood and stool)

Laboratory blood tests revealed elevated erythrocyte sedimentation rate (ESR) in CD compared to control patients (52.3 ± 43.2 vs. 7.0 ± 4.7 , $p = 0.0040$). However, C-reactive protein, haemoglobin levels, platelets and leucocytes did not show statistically significant differences between groups (all $p > 0.05$). Laboratory stool tests for calprotectin showed increased levels in CD compared to control patients (1068.1 ± 995.7 vs. 243.7 ± 384.1 , $p = 0.0340$).

3.2.3. Ultrasound

B-mode ultrasound images were scored with modified Limberg score. Herein, differences between groups were found in the terminal ileum between control and CD patients (0.2 ± 0.6 vs. 1.9 ± 1.5 , $p = 0.0155$) but not between CD and UC patients (1.9 ± 1.5 vs. 0.3 ± 0.5 , $p = 0.1531$). Scoring of the sigmoid colon did not show any statistically significant differences (all $p > 0.05$).

3.2.4. Endoscopy

White light endoscopy was rated by SES-CD score in CD compared to control patients. While the mean score in controls did not indicate inflammation, the mean score in CD patients corresponded to moderate inflammation (0.0 ± 0.0 vs. 8.3 ± 8.0 , $p = 0.0014$). UCEIS score was used in UC compared to control patients. Herein moderate inflammation was found in UC patients, too (0.1 ± 0.3 vs. 5.2 ± 1.5 , $p = 0.0001$).

3.2.5. Histopathology

Standard histological staining (HE) was performed on mucosal biopsy specimens from all patients. The terminal ileum was scored according to Riley score adopted for CD and Nancy score, the sigmoid colon according to Riley score adopted for UC and Nancy score, respectively. In the terminal ileum, a statistically increased Riley and Nancy score was found in CD compared to control patients (8.4 ± 5.6 vs. 0.3 ± 0.7 , $p = 0.0022$ and 2.4 ± 1.5 vs. 0.0 ± 0.0 , $p = 0.0006$). Similarly, in the sigmoid colon Riley and Nancy scores were elevated in UC compared to control patients (11.0 ± 7.1 vs. 0.5 ± 0.5 , $p = 0.0021$ and 2.8 ± 1.8 vs. 0.0 ± 0.0 , $p = 0.0028$). However, no statistically significant differences were found between CD and UC patients in the terminal ileum nor in the sigmoid colon.

3.2.6. Magnetic resonance (MR) enterography

Of all patients, $n = 11$ underwent MR-enterography (control patients $n = 2$, UC $n = 4$ and CD $n = 5$). sMaria scores, while increased, were not statistically significant in CD and UC patients compared to controls (1.6 ± 1.8 vs. 3.3 ± 5.9 vs. 0.5 ± 0.7 , all $p > 0.05$).

3.2.7. Multispectral Optoacoustic Tomography

For this purpose, two MSOT/RUCT scans of the terminal ileum and the sigmoid colon of each patient were analysed. Integrated RUCT

imaging allows anatomical guidance and identification of the bowel wall during handheld bedside MSOT imaging (Fig. 2a-c). By using multiple laser light wavelengths in the near-infrared range of light (NIR), deoxygenated (HbR) and oxygenated (HbO₂) haemoglobin can be visualized and then quantified by dedicated software (Fig. 2d). Exemplary MSOT images in comparison with standard assessments are displayed for the terminal ileum and the sigmoid colon in Fig. 3a+b and Supplementary Figure 1. Furthermore, MSOT parameters total haemoglobin (HbT) and MSOT-derived oxygen saturation (mSO₂) can be calculated. For comparison, MSOT signals at the isobestic point for haemoglobin (single wavelength 800 nm (SWL800)) are also depicted. The MSOT measures from the terminal ileum of two patients (control patients $n = 2$) and the sigmoid colon of 4 patients (control patient $n = 1$, UC $n = 1$, CD $n = 2$) had to be excluded due to attenuated or artefact-rich OAI signals.

In the terminal ileum SWL800, HbT and HbR were statistically significantly increased in CD compared to control patients. In detail, SWL800 was 13.7 ± 4.6 a.u. vs. 25.2 ± 3.0 a.u. ($p = 0.0103$), HbT was 32.9 ± 15.4 a.u. vs. 72.1 ± 13.0 a.u. ($p = 0.0049$) and HbR was 24.1 ± 13.1 a.u. vs. 50.0 ± 16.8 a.u. ($p = 0.0228$), respectively (Fig. 3c). The latter parameters did not show statistically significant differences between CD and UC patients. Furthermore, MSOT parameters HbO₂ and mSO₂ did not show statistically significant differences between all groups in the terminal ileum (all $p > 0.05$, Fig. 3c).

Comparing MSOT signal intensities between groups in the sigmoid colon, a statistically significant difference was found between control and UC patients for SWL800nm, HbT and HbO₂ as follows: SWL800 was 13.2 ± 4.5 a.u. vs. 23.5 ± 4.3 a.u. ($p = 0.228$), HbT was 35.1 ± 16.3 a.u. vs. 62.9 ± 13.8 a.u. ($p = 0.0311$) and HbO₂ was 7.6 ± 4.5 a.u. vs. 20.2 ± 7.5 a.u. ($p = 0.0162$) (Fig. 3d). Moreover, HbO₂ was also elevated in CD compared to control patients (7.6 ± 4.5 a.u. vs. 18.1 ± 9.8 a.u. ($p = 0.0412$)). MSOT parameter HbR and mSO₂ did not show relevant differences between groups (all $p > 0.05$, Fig. 3d).

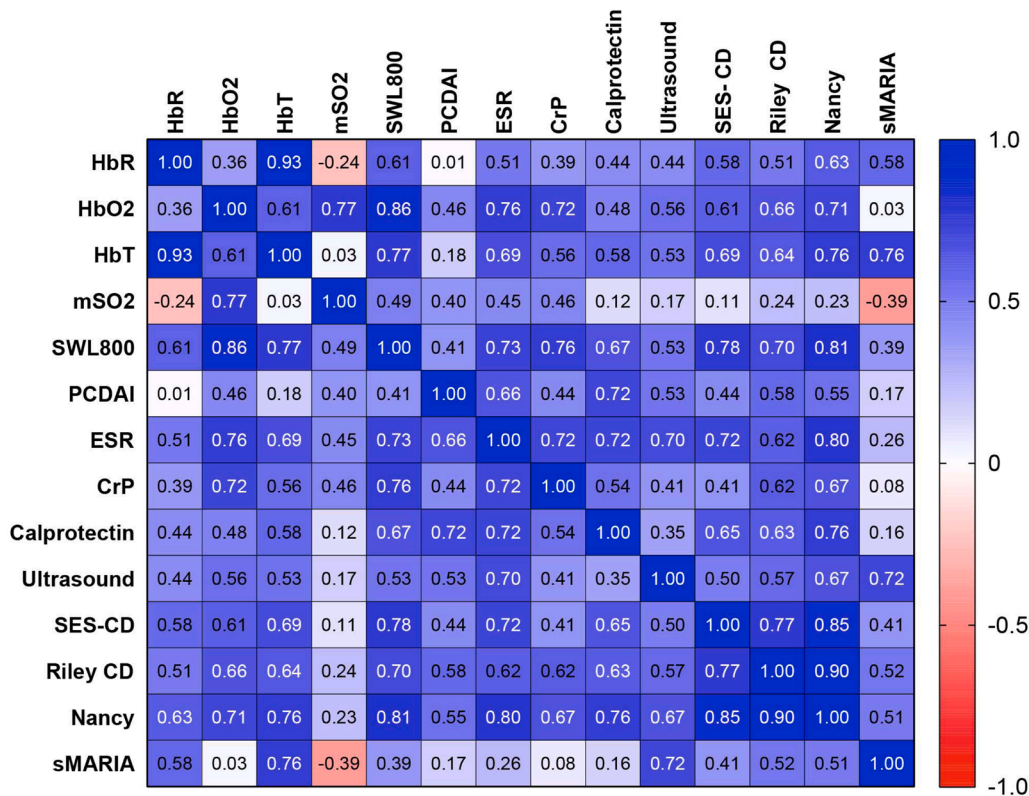
3.3. MSOT correlation with multimodal disease assessment

To evaluate the performance of MSOT in assessing disease severity in paediatric inflammatory bowel diseases, we correlated MSOT parameters with clinical, laboratory, ultrasound, endoscopic and MR-enterography scores.

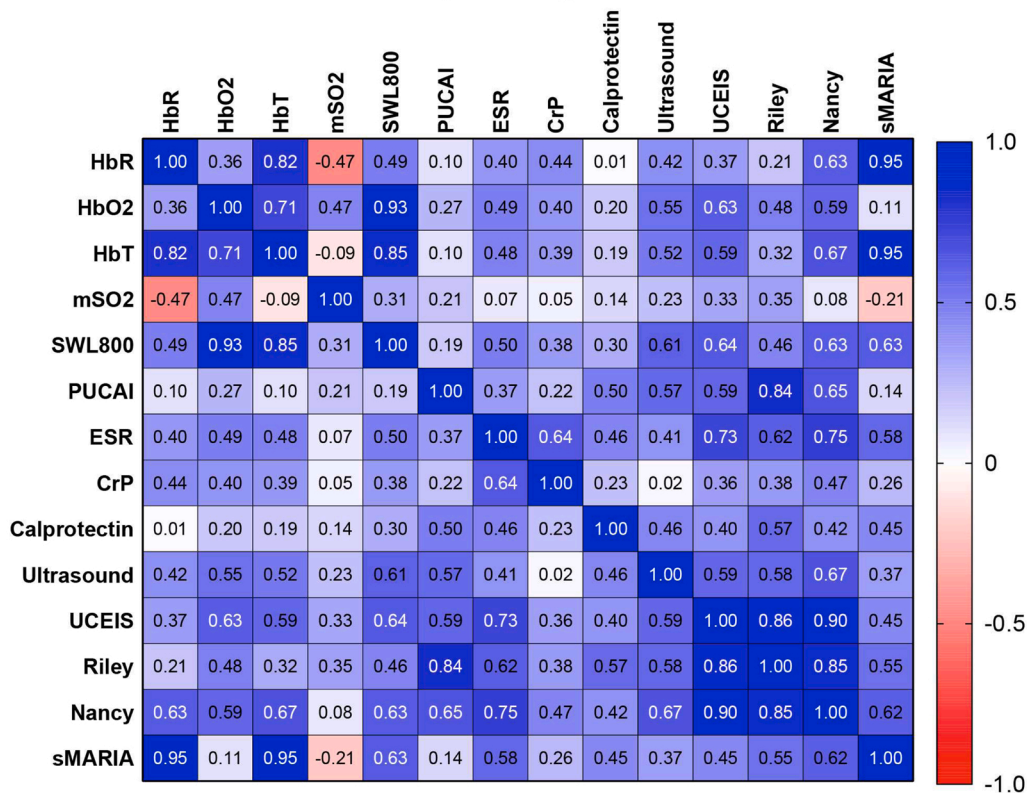
First, signal intensities of MSOT parameters of the terminal ileum of control and CD patients were correlated. Herein, no statistically significant correlation with clinical standard assessment (PCDAI) was found. However, laboratory parameters showed a significant correlation with different MSOT haemoglobin signals. ESR showed the statistically most significant positive correlation with HbO₂ ($rs=0.76$, $p = 0.0024$), CrP with SWL800 ($rs=0.76$, $p = 0.0017$) and calprotectin with SWL800 ($rs=0.67$, $p = 0.0147$). Furthermore, multimodal imaging revealed the highest correlation between ultrasound Limberg score and HbO₂ ($rs=0.56$, $p = 0.0338$) and between SES-CD and SWL800 ($rs=0.78$, $p = 0.0017$). No correlations between sMARIA score and MSOT parameters were found. Histological scoring showed the highest correlation between Riley score and SWL800 ($rs=0.70$, $p = 0.0101$) and between Nancy score and SWL800 ($rs=0.81$, $p = 0.0013$) (Fig. 4a).

Next, signal intensities of MSOT parameters of the sigmoid colon of control and UC patients were correlated. Again, no statistically

A Crohn's diseases and control patients - Terminal ileum



B Ulcerative colitis and control patients- Sigmoid colon



(caption on next page)

Fig. 4. Correlation of MSOT haemoglobin parameters and standard disease activity measures. HbR = Deoxygenated haemoglobin, HbO2 = oxygenated haemoglobin, mSO2 = oxygen saturation, HbT = total haemoglobin and SWL800nm = single wavelength 800 nm, PCDAI = Paediatric Crohn's Disease Activity Index, PUCAI = Paediatric Ulcerative Colitis Activity Index, ESR = Erythrocyte Sedimentation Rate, CrP = C-reactive protein, TI = terminal ileum, SI = sigmoid colon, SES-CD = simple endoscopic score for Crohn's disease, UCEIS = Ulcerative Colitis Endoscopic Index of Severity, sMARIA = simplified Magnetic Resonance Index of Activity (A+B) MSOT haemoglobin signal intensities of the terminal ileum of control and CD patients (A) and of the sigmoid colon of control and UC patients (B) were correlated with standard disease activity measures. In detail, MSOT signal intensities for HbR, HbO2, mSO2, HbT and SWL800nm were compared with laboratory measures (ESR, CrP, Calprotectin), sonographic Limberg score, endoscopic SES-CD/UCEIS score, histopathologic Riley and Nancy score and MR-enterographic sMARIA score. Given is the respective Spearman correlation coefficient.

significant correlation with clinical standard assessment (PUCAI) was found. Furthermore, no statistically significant correlation between MSOT parameters and laboratory blood (ESR, CrP) and stool (calprotectin) biomarkers for inflammation were observed (all $p > 0.05$). A statistically significant correlation with ultrasound Limberg score was found for MSOT HbO2 ($r_s=0.55$, $p = 0.0440$) and SWL800nm ($r_s=0.61$, $p = 0.0110$), UCEIS score and HbO2 ($r_s=0.63$, $p = 0.0193$) and SWL800 ($r_s=0.64$, $p = 0.0166$). No correlation with sMARIA score was found (all $p > 0.05$). Histological scoring, according to Riley score for UC, did not show a statistically significant correlation. Nancy score revealed a statistically significant correlation with SWL800nm, HbT, HbR and HbO2 (best for HbT: $r_s=0.67$, $p = 0.0140$) (Fig. 4b).

4. Discussion.

In this study of paediatric patients with IBD, we demonstrated the ability of MSOT to assess disease activity utilizing haemoglobin signal intensities in the intestinal walls. Compared to controls, CD patients showed increased signal levels in the terminal ileum and UC patients in the sigmoid colon, respectively. Both findings are well explained by the pathophysiology of the disease and the individual disease activity. Secondly, routine clinical assessment correlated well with MSOT haemoglobin parameters.

Until now, a single clinical, laboratory or non-invasive imaging modality for assessing the presence and, even better, the intensity of mucosal inflammation does not exist [5]. Especially novel, non-invasive imaging modalities might hold the promise to provide advanced measures to assess intestinal inflammation. In a first clinical trial, MSOT was already able to distinguish between remission and activity in CD, which outperformed other standard assessments [10]. While it is known that these patients often need to undergo invasive diagnostic procedures, children and adolescents in particular would benefit from the use of such non-invasive technologies. With regard to MSOT, studies in children with muscular disorders have demonstrated that imaging conditions might be optimal in such populations [23,24].

Although, OAI signals of the intestinal wall in children might be influenced from other light absorbing tissue components, especially the melanin rich skin and haemo/myoglobin rich muscle tissue, and reflectance artefacts, discrimination between groups was feasible with good correlation to standard assessments and in line with previous observations in adults [9,10]. Furthermore, in preclinical models of murine colitis elevated haemoglobin signals were attributed to the intestinal wall, too [35,36] and raster-scanning optoacoustic mesoscopy even enabled detailed mapping of the intestinal vascular networks [37]. Therefore, the changes in haemoglobin signals in our study were attributed to the intestinal wall, too. By using multiple wavelengths in the NIR to generate and quantify functional measures of deoxygenated and oxygenated haemoglobin, we were able to provide significant differences between healthy and diseased groups. The increase in total haemoglobin levels can be attributed to dilated vessels and augmented blood supply as signs of acute inflammation [38,39]. However, more differentiated, inflammation in the terminal ileum of CD patients was marked by means of elevated deoxygenated haemoglobin and in the sigmoid colon by increased oxygenated haemoglobin in CD and UC patients. In turn, mSO2 remained insignificant, which is most likely due to the current technical limitations [40] and might be resolved by the ongoing advances in data analyses [41,42]. However, other phantom, ex-vivo and in-vivo studies demonstrated high accuracy of multispectral analyses for hemoglobin parameters and blood oxygenation in comparison with gold standards in different scenarios, already [43–51]. For

the intestinal wall, no standard modality to assess the oxygen saturation or the ratio between oxygenated and deoxygenated haemoglobin exists. Pathophysiological, acute inflammation enhances hypoxia, leading to angiogenesis and hypervascularization, making it a potential therapeutic target in IBD [52]. Furthermore, Rigottier-Gois hypothesized that oxygen may play a significant role in IBD dysbiosis [53], making MSOT a promising tool in monitoring future treatment strategies. In contrast to a functional multiwavelength approach, the morphologic single wavelength imaging using 800 nm – the wavelength where both deoxygenated and oxygenated haemoglobin absorbs similarly (isosbestic point) – might be analogically capable to detect increased disease activity [54]. However, molecular decoding of different tissue components would allow further insights in the course of the disease and was already demonstrated in preclinical OAI approaches of murine colitis [35,37]. Currently, different approaches are followed to overcome the limitations of spectral unmixing in deep tissues by spectral coloring – the alteration of optoacoustic spectra by depth, used wavelengths and in respect of the biological tissue composition [14,42,55,56]. Current research in the field pose the potential of novel algorithms to overcome these issues [41, 42], and universally applicable data analysis strategies are matter of debate [57]. Future strategies include standardization of data acquisition, analysis and verification of pilot-studies in double-blind controlled trials, finally.

To verify the clinical value of MSOT for PIBD patients, we correlated MSOT haemoglobin values with routine standard assessments. In CD, MSOT SWL 800 nm showed the highest correlation with SES-CD score and the histopathological Nancy score. The correlation was even higher than for standard clinical and laboratory assessments. However, correlations of SES-CD with histopathological scores were highest. In UC patients, similar correlations were found between MSOT haemoglobin levels, UCEIS and standard clinical and laboratory assessments. Correlations with MR-enterography are limited to the very small number of participants. But, although specificity of MR-enterography is high, sensitivity is limited [58]. Furthermore, similar to MR-enterography, intestinal contrast agents might further enhance the visibility of the intestinal inflammation. Using orally administered indocyanine green, MSOT would be capable to depict gastro-intestinal transit in real-time [59]. Similar applications in IBD patients could be used to diagnose intestinal complications, such as strictures or fistulas, and might allow targeted therapeutical approaches.

Our study is limited by the small sample size, so that no stratification according to disease severity was reliable. However, we provide the first dataset on paediatric IBD compared to control patients, which serves as a basis for following larger studies in paediatric IBD. MSOT is further limited by imaging depth and influential factors such as bowel movement and air filling. However, first data on the precision of MSOT for longitudinal assessment of the intestine showed that physiological conditions such as sex and postprandial increased blood flow do not alter the OAI haemoglobin signals [60]. However, imaging depth partially correlates with signal intensities [25,60] and might be improved by advanced depth correction algorithms [61].

In conclusion, we showed that MSOT may serve as a novel monitoring tool for paediatric IBD patients. Further studies are needed.

Funding

This work was supported by the Interdisciplinary Center for Clinical

Research (IZKF) at the University Hospital of the Friedrich-Alexander-Universität (FAU) [J89 and Clinician Scientist Program to APR].

Declaration of Competing Interest

The authors declare the following financial interests/personal relationships which may be considered as potential competing interests. Markus F Neurath, Maximilian J Waldner, Ferdinand Knieling reports financial support was provided by European Union. Adrian P Regensburger reports financial support was provided by Friedrich Alexander University Erlangen Nuremberg Faculty of Medicine. Adrian P Regensburger, Ferdinand Knieling, Maximilian J Waldner has patent issued to iThera Medical GmbH, Munich, Germany. Ferdinand Knieling is a section editor of the Journal Photoacoustics, however not involved in the peer review process of this manuscript.

Data availability

Data will be made available on request.

Acknowledgement

The present work was performed in (partial) fulfilment of the requirements for obtaining the degree “Dr. rer. biol. hum.” for APR at the Friedrich-Alexander-Universität Erlangen-Nürnberg (FAU).

We thank the Team of the Department of paediatric gastroenterology for their support, especially Cristina Kreissl, Victoria Schwarzmayr, Stefan Zimmermann and Margit Schmid.

We thank Yi Qiu and Claudia Jendrewski from iThera medical GmbH (Munich Germany) for technical specifications in the methods section.

Conflicts of interest

APR, MJW and FK are shared patent holders together with iThera Medical GmbH (Munich, Germany) on the optoacoustic imaging system/software described in the study. FK is a section editor of the journal, but not involved in the peer review of this manuscript.

Author contribution

APR and FK conceived the idea of the study. APR and FK were the principle investigators. APR, LPP, RR and FK performed MSOT imaging. APR and JJ performed ultrasound imaging. APR, AR and AH performed endoscopic procedures and scoring. ME performed histopathologic scoring. MW performed MRI scoring. APR, MJW, AH and FK performed (statistical) data analysis. APR, ME, MW, AB, EN, VD, ALW, AS, UR, OR, MU, AH, MFN, MJW, AH and FK interpreted the data. APR wrote the first draft of the manuscript. All other authors revised it critically with all aspects of intellectual content and approved the final version of the manuscript.

Appendix A. Supporting information

Supplementary data associated with this article can be found in the online version at [doi:10.1016/j.pacs.2023.100578](https://doi.org/10.1016/j.pacs.2023.100578).

References

- [1] E.I. Benchimol, K.J. Fortinsky, P. Gozdyra, M. Van den Heuvel, J. Van Limbergen, A.M. Griffiths, Epidemiology of pediatric inflammatory bowel disease: a systematic review of international trends, *Inflamm. Bowel Dis.* 17 (1) (2011) 423–439.
- [2] J. Sýkora, R. Pomahačová, M. Kreslová, D. Cvalínová, P. Stych, J. Schwarz, Current global trends in the incidence of pediatric-onset inflammatory bowel disease, *World J. Gastroenterol.* 24 (25) (2018) 2741–2763.
- [3] K.A. Diefenbach, C.K. Breuer, Pediatric inflammatory bowel disease, *World J. Gastroenterol.: WJG* 12 (20) (2006) 3204–3212.
- [4] L. Peyrin-Biroulet, M. Ferrante, F. Magro, S. Campbell, D. Franchimont, H. Fidder, H. Strid, S. Ardizzone, G. Veereman-Wauters, J.-B. Chevaux, M. Allez, S. Danese,

- A. Sturm, Results from the 2nd Scientific Workshop of the ECCO (I): Impact of mucosal healing on the course of inflammatory bowel disease, *J. Crohn's. Colitis* 5 (5) (2011) 477–483.
- [5] F.M. Ruemmele, J.S. Hyams, A. Otley, A. Griffiths, K.-L. Kolho, J.A. Dias, A. Levine, J.C. Escher, J. Taminiau, G. Veres, J.-F. Colombel, S. Vermeire, D.C. Wilson, D. Turner, Outcome measures for clinical trials in paediatric IBD: an evidence-based, expert-driven practical statement paper of the paediatric ECCO committee, *Gut* 64 (3) (2015) 438–446.
- [6] A. Heida, K.T. Park, P.F. van Rheenen, Clinical Utility of Fecal Calprotectin Monitoring in Asymptomatic Patients with Inflammatory Bowel Disease: A Systematic Review and Practical Guide, *Inflamm. Bowel Dis.* 23 (6) (2017) 894–902.
- [7] M.T. Dolinger, M. Kayal, Intestinal ultrasound as a non-invasive tool to monitor inflammatory bowel disease activity and guide clinical decision making, *World J. Gastroenterol.: WJG* 29 (15) (2023) 2272–2282.
- [8] R. B. Herman, P. Dumnicka, K. Fyderek, A review of magnetic resonance enterography based Crohn's disease activity indices in paediatric patients, *Prz. Gastroenterol.* 17 (3) (2022) 190–195.
- [9] M.J. Waldner, F. Knieling, C. Egger, S. Morscher, J. Claussen, M. Vetter, C. Kielisch, S. Fischer, L. Pfeifer, A. Hagel, R.S. Goertz, D. Wildner, R. Atreya, D. Strobel, M. F. Neurath, Multispectral Optoacoustic Tomography in Crohn's Disease: Noninvasive Imaging of Disease Activity, *Gastroenterology* 151 (2) (2016) 238–240.
- [10] F. Knieling, C. Neufert, A. Hartmann, J. Claussen, A. Urich, C. Egger, M. Vetter, S. Fischer, L. Pfeifer, A. Hagel, C. Kielisch, R.S. Gortz, D. Wildner, M. Engel, J. Rother, W. Uter, J. Siebler, R. Atreya, W. Rascher, D. Strobel, M.F. Neurath, M. J. Waldner, Multispectral Optoacoustic Tomography for Assessment of Crohn's Disease Activity, *N. Engl. J. Med* 376 (13) (2017) 1292–1294.
- [11] V. Ntziachristos, D. Razansky, Molecular imaging by means of multispectral optoacoustic tomography (MSOT), *Chem. Rev.* 110 (5) (2010) 2783–2794.
- [12] L.V. Wang, S. Hu, Photoacoustic tomography: in vivo imaging from organelles to organs, *Science* 335 (6075) (2012) 1458–1462.
- [13] L.V. Wang, J. Yao, A practical guide to photoacoustic tomography in the life sciences, *Nat. Methods* 13 (8) (2016) 627–638.
- [14] S. Tzoumas, N. Deliolanis, S. Morscher, V. Ntziachristos, Unmixing Molecular Agents From Absorbing Tissue in Multispectral Optoacoustic Tomography, *IEEE Trans. Med. Imaging* 33 (1) (2014) 48–60.
- [15] A.P. Regensburger, E. Brown, G. Kronke, M.J. Waldner, F. Knieling, Optoacoustic Imaging in Inflammation, *Biomedicine* 9 (5) (2021).
- [16] D.J. Waterhouse, S. Bano, W. Januszewicz, D. Stoyanov, R.C. Fitzgerald, M. di Pietro, S.E. Bohndiek, First-in-human pilot study of snapshot multispectral endoscopy for early detection of Barrett's-related neoplasia, *J. Biomed. Opt.* 26 (10) (2021).
- [17] J.M. Yang, C. Favazza, R. Chen, J. Yao, X. Cai, K. Maslov, Q. Zhou, K.K. Shung, L. V. Wang, Simultaneous functional photoacoustic and ultrasonic endoscopy of internal organs in vivo, *Nat. Med* 18 (8) (2012) 1297–1302.
- [18] H. He, A. Styliogiannis, P. Afshari, T. Wiedemann, K. Steiger, A. Buehler, C. Zakian, V. Ntziachristos, Capsule optoacoustic endoscopy for esophageal imaging, *J. Biophotonics* 12 (10) (2019), e201800439.
- [19] J. Hyams, J. Markowitz, A. Otley, J. Rosh, D. Mack, A. Bousvaros, S. Kugathasan, M. Pfefferkorn, V. Tolia, J. Evans, W. Treem, R. Wyllie, R. Rothbaum, J. del Rosario, A. Katz, A. Mezoff, M. Oliva-Hemker, T. Lerer, A. Griffiths, G. Pediatric Inflammatory Bowel Disease Collaborative Research, Evaluation of the pediatric crohn disease activity index: a prospective multicenter experience, *J. Pediatr Gastroenterol. Nutr.* 41 (4) (2005) 416–421.
- [20] J.S. Hyams, G.D. Ferry, F.S. Mandel, J.D. Gryboski, P.M. Kibort, B.S. Kirschner, A. M. Griffiths, A.J. Katz, R.J. Grand, J.T. Boyle, et al., Development and validation of a pediatric Crohn's disease activity index, *J. Pediatr Gastroenterol. Nutr.* 12 (4) (1991) 439–447.
- [21] D. Turner, A.R. Otley, D. Mack, J. Hyams, J. de Bruijne, K. Uusoue, T.D. Walters, M. Zachos, P. Mamula, D.E. Beaton, A.H. Steinhart, A.M. Griffiths, Development, validation, and evaluation of a pediatric ulcerative colitis activity index: a prospective multicenter study, *Gastroenterology* 133 (2) (2007) 423–432.
- [22] B. Limberg, [Diagnosis of chronic inflammatory bowel disease by ultrasonography], *Z. fur Gastroenterol.* 37 (6) (1999) 495–508.
- [23] A.P. Regensburger, L.M. Fonteyne, J. Jungert, A.L. Wagner, T. Gerhalter, A. M. Nagel, R. Heiss, F. Flenkenthaler, M. Qurashi, M.F. Neurath, N. Klymiuk, E. Kemter, T. Frohlich, M. Uder, J. Woelfle, W. Rascher, R. Trollmann, E. Wolf, M. J. Waldner, F. Knieling, Detection of collagens by multispectral optoacoustic tomography as an imaging biomarker for Duchenne muscular dystrophy, *Nat. Med* 25 (12) (2019) 1905–1915.
- [24] A.P. Regensburger, A.L. Wagner, V. Danko, J. Jungert, A. Federle, D. Klett, S. Schuessler, A. Buehler, M.F. Neurath, A. Roos, H. Lochmuller, J. Woelfle, R. Trollmann, M.J. Waldner, F. Knieling, Multispectral optoacoustic tomography for non-invasive disease phenotyping in pediatric spinal muscular atrophy patients, *Photoacoustics* 25 (2022), 100315.
- [25] A.L. Wagner, V. Danko, A. Federle, D. Klett, D. Simon, R. Heiss, J. Jungert, M. Uder, G. Schett, M.F. Neurath, J. Woelfle, M.J. Waldner, R. Trollmann, A. P. Regensburger, F. Knieling, Precision of handheld multispectral optoacoustic tomography for muscle imaging, *Photoacoustics* 21 (2021), 100220.
- [26] E. Mercep, G. Jeng, S. Morscher, P.C. Li, D. Razansky, Hybrid optoacoustic tomography and pulse-echo ultrasonography using concave arrays, *IEEE Trans. Ultrason. Ferroelectr. Freq. Control* 62 (9) (2015) 1651–1661.
- [27] J. Rimola, S. Rodriguez, O. Garcia-Bosch, I. Ordas, E. Ayala, M. Aceituno, M. Pellise, C. Ayuso, E. Ricart, L. Donoso, J. Panes, Magnetic resonance for

- assessment of disease activity and severity in ileocolonic Crohn's disease, *Gut* 58 (8) (2009) 1113–1120.
- [28] I. Ordas, J. Rimola, I. Alfaro, S. Rodriguez, J. Castro-Poceiro, A. Ramirez-Morros, M. Gallego, A. Giner, R. Barastegui, A. Fernandez-Clotet, M. Masamunt, E. Ricart, J. Panes, Development and Validation of a Simplified Magnetic Resonance Index of Activity for Crohn's Disease, *Gastroenterology* 157 (2) (2019) 432–439, e1.
- [29] M. Daperno, G. D'Haens, G. Van Assche, F. Baert, P. Bulois, V. Maunoury, R. Sostegni, R. Rocca, A. Pera, A. Gevers, J.Y. Mary, J.F. Colombel, P. Rutgeerts, Development and validation of a new, simplified endoscopic activity score for Crohn's disease: the SES-CD, *Gastrointest. Endosc.* 60 (4) (2004) 505–512.
- [30] L. Vuitton, P. Marteau, W.J. Sandborn, B.G. Levesque, B. Feagan, S. Vermeire, S. Danese, G. D'Haens, M. Lowenberg, R. Khanna, G. Fiorino, S. Travis, J.Y. Mary, L. Peyrin-Biroulet, IOIBD technical review on endoscopic indices for Crohn's disease clinical trials, *Gut* 65 (9) (2016) 1447–1455.
- [31] S.P. Travis, D. Schnell, P. Krzeski, M.T. Abreu, D.G. Altman, J.F. Colombel, B. G. Feagan, S.B. Hanauer, M. Lemann, G.R. Lichtenstein, P.R. Marteau, V. Reinisch, B.E. Sands, B.R. Yacyshyn, C.A. Bernhardt, J.Y. Mary, W.J. Sandborn, Developing an instrument to assess the endoscopic severity of ulcerative colitis: the Ulcerative Colitis Endoscopic Index of Severity (UCEIS), *Gut* 61 (4) (2012) 535–542.
- [32] K. Ikeya, H. Hanai, K. Sugimoto, S. Osawa, S. Kawasaki, T. Iida, Y. Maruyama, F. Watanabe, The Ulcerative Colitis Endoscopic Index of Severity More Accurately Reflects Clinical Outcomes and Long-term Prognosis than the Mayo Endoscopic Score, *J. Crohns Colitis* 10 (3) (2016) 286–295.
- [33] S.A. Riley, V. Mani, M.J. Goodman, S. Dutt, M.E. Herd, Microscopic activity in ulcerative colitis: what does it mean? *Gut* 32 (2) (1991) 174–178.
- [34] A. Marchal-Bressenot, J. Salleron, C. Boulagnon-Rombi, C. Bastien, V. Cahn, G. Cadot, M.D. Diebold, S. Danese, W. Reinisch, S. Schreiber, S. Travis, L. Peyrin-Biroulet, Development and validation of the Nancy histological index for UC, *Gut* 66 (1) (2017) 43–49.
- [35] N. Bhatiani, W.E. Grizzle, S. Galandiuk, D. O'tali, G.W. Dryden, N.K. Egilmez, L. R. McNally, Noninvasive Imaging of Colitis Using Multispectral Optoacoustic Tomography, *J. Nucl. Med* 58 (6) (2017) 1009–1012.
- [36] F. Knieling, J. Gonzales Menezes, J. Claussen, M. Schwarz, C. Neufert, F. B. Fahlbusch, T. Rath, O.M. Thoma, V. Kramer, B. Menchicchi, C. Kersten, K. Scheibe, S. Schürmann, B. Carlé, W. Rascher, M.F. Neurath, V. Ntziachristos, M. J. Waldner, Raster-Scanning Optoacoustic Mesoscopy for Gastrointestinal Imaging at High Resolution, *Gastroenterology* 154 (4) (2018) 807–809.e3.
- [37] A. Buehler, E. Brown, L.P. Paulus, M. Eckstein, O.M. Thoma, M.E. Oraipoulou, U. Rother, A. Hoerning, A. Hartmann, M.F. Neurath, J. Woelfle, O. Friedrich, M. J. Waldner, F. Knieling, S.E. Bohndiek, A.P. Regensburger, Transrectal Absorber Guide Raster-Scanning Optoacoustic Mesoscopy for Label-Free In Vivo Assessment of Colitis, *Adv. Sci. (Weinh.)* (2023), e2300564.
- [38] L. Hultén, J. Lindhagen, O. Lundgren, S. Fasth, C. Åhrén, Regional intestinal blood flow in ulcerative colitis and Crohn's disease, *Gastroenterology* 72 (3) (1977) 388–396.
- [39] T.J. Williams, M.J. Peck, Role of prostaglandin-mediated vasodilatation in inflammation, *Nature* 270 (5637) (1977) 530–532.
- [40] M. Gehrung, S.E. Bohndiek, J. Brunker, Development of a blood oxygenation phantom for photoacoustic tomography combined with online pO₂ detection and flow spectrometry, *J. Biomed. Opt.* 24 (12) (2019) 1–11.
- [41] J. Grohl, T. Kirchner, T.J. Adler, L. Hacker, N. Holzwarth, A. Hernandez-Aguilera, M.A. Herrera, E. Santos, S.E. Bohndiek, L. Maier-Hein, Learned spectral decoloring enables photoacoustic oximetry, *Sci. Rep.* 11 (1) (2021), 6565.
- [42] V. Grasso, H.W. Hassan, P. Mirtaheri, R. Willumeit-Römer, J. Jose, Recent advances in photoacoustic blind source spectral unmixing approaches and the enhanced detection of endogenous tissue chromophores, *Front. Signal Process.* 2 (2022).
- [43] X. Wang, X. Xie, G. Ku, L.V. Wang, G. Stoica, Noninvasive imaging of hemoglobin concentration and oxygenation in the rat brain using high-resolution photoacoustic tomography, *J. Biomed. Opt.* 11 (2) (2006), 024015.
- [44] W.C. Vogt, X. Zhou, R. Andriani, K.A. Wear, T.J. Pfefer, B.S. Garra, Photoacoustic oximetry imaging performance evaluation using dynamic blood flow phantoms with tunable oxygen saturation, *Biomed. Opt. Express* 10 (2) (2019) 449–464.
- [45] T. Mitcham, H. Taghavi, J. Long, C. Wood, D. Fuentes, W. Stefan, J. Ward, R. Bouchard, Photoacoustic-based SO estimation through excised bovine prostate tissue with interstitial light delivery, in: *Photoacoustics*, 7, 2017, pp. 47–56.
- [46] J.G. Yang, G. Zhang, W. Chang, Z.H. Chi, Q.Q. Shang, M. Wu, T. Pan, L. Huang, H. B. Jiang, Photoacoustic imaging of hemodynamic changes in forearm skeletal muscle during cuff occlusion, *Biomed. Opt. Express* 11 (8) (2020) 4560–4570.
- [47] S.R. Liu, R. Zhang, T. Han, Y.H. Pan, G.J. Zhang, X. Long, C.Y. Zhao, M. Wang, X. L. Li, F. Yang, Y.C. Sang, L. Zhu, X.J. He, J.C. Li, Y.W. Zhang, C.H. Li, Y.X. Jiang, M. Yang, Validation of photoacoustic/ultrasound dual imaging in evaluating blood oxygen saturation, *Biomed. Opt. Express* 13 (10) (2022) 5551–5570.
- [48] R.O. Esenaliev, Y.Y. Petrov, O. Hartrumpf, D.J. Deyo, D.S. Prough, Continuous, noninvasive monitoring of total hemoglobin concentration by an optoacoustic technique, *Appl. Opt.* 43 (17) (2004) 3401–3407.
- [49] L. Hacker, J. Brunker, E.S.J. Smith, I. Quiros-Gonzalez, S.E. Bohndiek, Photoacoustics resolves species-specific differences in hemoglobin concentration and oxygenation, *J. Biomed. Opt.* 25 (9) (2020).
- [50] J.S. Günther, F. Knieling, A.P. Träger, W. Lang, A. Meyer, A.P. Regensburger, A. L. Wagner, R. Trollmann, J. Woelfle, D. Klett, W. Uter, M. Uder, M.F. Neurath, M. J. Waldner, U. Rother, Targeting Muscular Hemoglobin Content for Classification of Peripheral Arterial Disease by Noninvasive Multispectral Optoacoustic Tomography, *JACC Cardiovasc Imaging* 16 (5) (2023) 719–721.
- [51] A. Karlas, N.A. Fasoula, K. Paul-Yuan, J. Reber, M. Kallmayer, D. Bozhko, M. Seeger, H.H. Eckstein, M. Wildgruber, V. Ntziachristos, Cardiovascular optoacoustics: From mice to men - A review, *Photoacoustics* 14 (2019) 19–30.
- [52] L.E. Glover, S.P. Colgan, Hypoxia and metabolic factors that influence inflammatory bowel disease pathogenesis, *Gastroenterology* 140 (6) (2011) 1748–1755.
- [53] L. Rigottier-Gois, Dysbiosis in inflammatory bowel diseases: the oxygen hypothesis, *Isme J.* 7 (7) (2013) 1256–1261.
- [54] S. Tzoumas, V. Ntziachristos, Spectral unmixing techniques for optoacoustic imaging of tissue pathophysiology, *Philosophical Transactions of the Royal Society A: Mathematical (2017)*, *Phys. Eng. Sci.* 375 (2107) (2017) 0262.
- [55] J.P. Fuenzalida Werner, Y. Huang, K. Mishra, R. Janowski, P. Vetschera, C. Heichler, A. Chmyrov, C. Neufert, D. Niessing, V. Ntziachristos, A.C. Stiel, Challenging a Preconception: Optoacoustic Spectrum Differs from the Optical Absorption Spectrum of Proteins and Dyes for Molecular Imaging, *Anal. Chem.* 92 (15) (2020) 10717–10724.
- [56] B. Cox, J.G. Laufer, S.R. Arridge, P.C. Beard, Quantitative spectroscopic photoacoustic imaging: a review, *J. Biomed. Opt.* 17 (6) (2012), 061202.
- [57] H. Assi, R. Cao, M. Castelino, B. Cox, F.J. Gilbert, J. Gröhl, K. Gurusamy, L. Hacker, A.M. Ivory, J. Joseph, F. Knieling, M.J. Leahy, L. Lilaj, S. Manohar, I. Meglinski, C. Moran, A. Murray, A.A. Oraevsky, M.D. Pagel, M. Pramanik, J. Raymond, M.K. A. Singh, W.C. Vogt, L. Wang, S. Yang, I. Members of, S.E. Bohndiek, A review of a strategic roadmapping exercise to advance clinical translation of photoacoustic imaging: From current barriers to future adoption, *Photoacoustics* 32 (2023), 100539.
- [58] M. Chavoshi, S.A. Mirshahvalad, A. Kasaean, S. Djalalinia, S. Kolahdoozan, A. R. Radmard, Diagnostic Accuracy of Magnetic Resonance Enterography in the Evaluation of Colonic Abnormalities in Crohn's Disease: A Systematic Review and Meta-Analysis, *Acad. Radio.* 28 (Suppl 1) (2021) S192–s202.
- [59] L.P. Paulus, A. Buehler, A.L. Wagner, R. Raming, J. Jungert, D. Simon, K. Tascilar, A. Schnell, U. Rother, M. Eckstein, W. Lang, A. Hoerning, G. Schett, M.F. Neurath, M.J. Waldner, R. Trollmann, J. Woelfle, S.E. Bohndiek, A.P. Regensburger, F. Knieling, Contrast-Enhanced Multispectral Optoacoustic Tomography for Functional Assessment of the Gastrointestinal Tract, *Adv. Sci. (Weinh.)* (2023), e2302562.
- [60] L.P. Paulus, A.L. Wagner, A. Buehler, R. Raming, J. Jungert, D. Simon, K. Tascilar, A. Schnell, J. Gunther, U. Rother, W. Lang, A. Hoerning, G. Schett, M.F. Neurath, J. Woelfle, M.J. Waldner, F. Knieling, A.P. Regensburger, Multispectral optoacoustic tomography of the human intestine - temporal precision and the influence of postprandial gastrointestinal blood flow, *Photoacoustics* 30 (2023), 100457.
- [61] J. Vonk, J. Kukacka, P.J. Steinkamp, J.G. de Wit, F.J. Voskuil, W.T. R. Hooghiemstra, M. Bader, D. Justel, V. Ntziachristos, G.M. van Dam, M.J. H. Wijtes, Multispectral optoacoustic tomography for in vivo detection of lymph node metastases in oral cancer patients using an EGFR-targeted contrast agent and intrinsic tissue contrast: A proof-of-concept study, *Photoacoustics* 26 (2022), 100362.



Dr. Adrian P. Regensburger is a clinician scientist at the Department of Pediatric and Adolescent Medicine at the University Hospital Erlangen and the Pediatric and Experimental Imaging Laboratory. He is consultant of the pediatric Department of Gastroenterology and Hepatology with special interest to inflammatory bowel diseases and the application of novel imaging modalities.



Dr. Ferdinand Knieling is a clinician scientist at the Department of Pediatric and Adolescent Medicine at the University Hospital Erlangen and the PI of the Pediatric and Experimental Imaging Laboratory. He is consultant of the pediatric Department of Neurology and one of the leading scientists in applied translational optoacoustic imaging.